Please do not adjust margins

The influence of nitrogen position on charge carrier mobility in enantiopure aza[6]helicene crystals

Received 00th January 20xx,
Accepted 00th January 20xx

DOI: 10.1039/x0xx00000x

www.rsc.org/

Francesco Salerno,[a,c] Beth Rice,[b,c] Julia A. Schmidt,[a] Matthew J. Fuchter,[a,c] Jenny Nelson,[b,c] and Kim E. Jelfs[a,c]*

The properties of an organic semiconductor are dependent on both the chemical structure of the molecule involved, and how it is arranged in the solid-state. It is challenging to extract the influence of each individual factor, as small changes in the molecular structure often dramatically change the crystal packing and hence solid-state structure. Here, we use calculations to explore the influence of the nitrogen position on the charge mobility of a chiral organic molecule when the crystal packing is kept constant. The transfer integrals for a series of enantiopure aza[6]helicene crystals sharing the same packing were analysed in order to identify the best supramolecular motifs to promote charge carrier mobility. The regioisomers considered differ only in the positioning of the nitrogen atom in the aromatic scaffold. The simulations showed that even this small change in the chemical structure has a strong effect on the charge transport in the crystal, leading to differences in charge mobility of up to one order of magnitude. Some aza[6]helicene isomers that were packed *interlocked* with each other showed high HOMO-HOMO integrals (up to 70 meV), whilst molecules arranged with *translational* symmetry generally afforded the highest LUMO-LUMO integrals (40 - 70 meV). As many of the results are not intuitively obvious, a computational approach provides additional insight into the design of new semiconducting organic materials.

Introduction

Organic molecules are finding increasing application as semiconductors in commercial electronic devices, from field-effect transistors to light-emitting diodes. The first requirement for these molecules is the effective transport of charge carriers when the molecules are processed into thin films. In this regard, the influence of solid-state packing on charge mobility is well known, but difficult to predict.[1,2] Charge mobility in small molecule-based electronic devices is generally improved by π-stacking interactions between aromatic cores of neighbouring units. The relative arrangement of the molecules in the solid-state is indeed a central aspect to consider. In turn, the supramolecular packing is influenced by the chemical structure of the single unit. These two intertwined aspects have been studied over the years, experimentally and theoretically, particularly for some typical classes of 'flat' molecules, such as pentacenes.[3,4]

Molecules that have 'twisted' or 'skewed' aromatic scaffolds potentially can have more complex structure-property relationships than 'flat' molecules. Helicene molecules are ortho-fused polycyclic aromatic molecules that are particularly interesting because of the helical nature of the core, which is intrinsically chiral. A chiral molecule exists in opposite forms, called enantiomers, which have the same molecular properties but interact differently with other chiral objects. Chirality has recently proven to be useful in organic electronics and spintronics.[5,6] Helicenes have always been a popular representative in chirality research for their helical shape and remarkable chiroptical properties, such as optical activity and circular dichroism.[7] Helicenes have been studied for application in asymmetric catalysis, liquid crystals, chemosensors and as stereoselective charge transfer complexes.[7–9] In the last decade, their use as organic semiconductors has been rather limited,[10–18] but is increasing and includes growing interest in extended twisted aromatic structures.[19]

Potentially, chirality adds a further variable that can influence the properties of organic semiconductors. Ensembles made from different compositions of the two enantiomers can form a variety of solid-state packings and the implications for electronic devices can be considerable, as recently shown for helicene-based organic field effect transistors (OFETs).[14] In another example involving an azaborahelicene,[15] the authors observed a charge carrier inversion whereby the hole mobility was high in the enantiopure crystal and the electron mobility high in the racemic crystal. This was a result of completely different solid-state packing in the enantiopure and racemic materials. To design new helicenes to be employed efficiently in optoelectronic devices, one of the aspects to understand is the relationship between chemical structure, chiral composition[14] (*i.e.* proportion of each enantiomer present), molecular packing and charge mobility.

So far, chemists have been guided mainly by their chemical 'intuition' in the design of new helicenes with defined supramolecular assemblies, using molecular structure to drive the molecules towards desired arrangements via intermolecular interactions.[20–23] However, the solid-state structure of aromatic organic molecules often depends on the interplay of weak van der Waals forces and thus the crystal packing can be hard to predict *a priori*, particularly beyond 'flat' arene molecules. In this regard, crystal structure prediction (CSP) of the solid-state packing of organic molecules can play a decisive role. CSP allows one to determine the most thermodynamically stable polymorphs given the chemical structure of the single molecule.[24] CSP has been combined with the prediction of optoelectronic properties to develop energy-structure-function (ESF) maps.[25–27] These maps have been applied, for instance, to understand the impact of different

[a] *Department of Chemistry, Imperial College London, White City Campus, London W12 0BZ, UK. Email: k.jelfs@imperial.ac.uk*
[b] *Department of Physics, Imperial College London, South Kensington Campus, London SW7 2AZ, UK.*
[c] *Centre for Plastic Electronics, Imperial College London, South Kensington Campus, London SW7 2AZ, UK.*
Electronic Supplementary Information (ESI) available. See DOI: 10.1039/x0xx00000x

Please do not adjust margins

packing on the charge mobility of unknown azapentacene derivatives.[26] The data confirmed that packings which maximized the π-π stacking interactions (sheet-like arrangements) also improved the charge transport and that these packings can be induced by C-H···N bonding. We have recently applied CSP to assist in the structure determination of 1-aza[6]helicene thin films, and explain the observed 80-fold difference in charge mobility between enantiopure and racemic material.[14] In a purely computational study, we explored the ESF map of the unsubstituted [6]carbohelicene using CSP.[28] We found that adjacent translational chains and herringbone translational homochiral chains of [6]helicenes were particularly efficient to promote high electron and hole mobility respectively. Whilst this prior study allowed us to unravel the influence of helicene crystal packing alone on charge mobility (as we used the same molecule throughout), here we focus on the influence of the molecular structure – specifically the position of the nitrogen atom within the ring – given the same crystal packing structure.

One of the aspects that emerged from our previous CSP studies is that a particular enantiopure polymorph is lowest energy for [6]helicenes, including [6]carbohelicene and 1-aza[6]helicene. A search of the Cambridge Structural Database (CSD) showed that other enantiopure aza[6]helicenes, namely 2-aza[6]helicene[29] and 6-aza[6]helicene[30] (where a nitrogen substitutes the C-H vertex in position 2 and 6 respectively) were found to crystallize in the same $P2_12_12_1$ space group, with identical packing features. Four molecules are contained in the unit cell. The crystal packing of 6-aza[6]helicene (CSD code PIHDOB) is shown in Figure 1. These observations support the assumption that the nitrogen position does not strongly influence the solid-state packing of the enantiopure [6]helicene crystal. However, the bulk optoelectronic properties should in principle vary depending on the different localization of the frontier orbitals, which are polarized by the electronegative nitrogen atom.

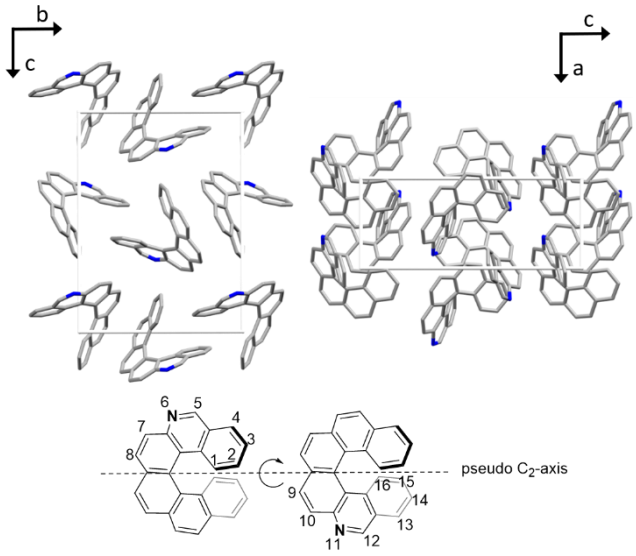


Figure 1. Top: two views of the crystal packing of (M)-6-aza[6]helicene (CSD code: PIHDOB). Carbons are shown in grey, nitrogens in blue and hydrogens omitted. Bottom: numbering of the carbon positions in the helicene scaffold considering the non-equivalence in the crystal cell after C_2 rotation.

In this work, we computationally study the effect of the nitrogen position on the transfer integrals and charge mobility for this specific helicene packing. We generate hypothetical packings of the low energy $P2_12_12_1$ enantiopure aza[6]helicene polymorph with different nitrogen positions. For each of these cells, the closest helicene pairs were analysed in order to identify the supramolecular motifs that contribute the most and the least to high transfer integrals and charge mobility in the crystal. We have attempted to rationalise our data guided by the principle that higher transfer integrals between two molecules derives from higher overlap of the frontier orbitals (HOMO-HOMO or LUMO-LUMO, for hole or electron transfer). The correlation between integrals of specific motifs and charge mobility of the whole cell is not always intuitive and will be discussed on a case by case basis. We found that some dimer motifs are particularly sensitive to the nitrogen position and tend to favour electron over hole mobility or *vice versa*. This knowledge could be exploited in crystal engineering to develop helicene systems with improved charge transport.

Methods

General procedure. Eight regioisomers of monoaza[6]helicene were considered in this study, each one corresponding to the substitution of a C-H vertex with a nitrogen atom. For comparison, we also added two additional chemical structures, the carbo[6]helicene and the 1,16-diaza[6]helicene. A further level of complexity arises from the pseudo-C_2 symmetry of the monoaza[6]helicenes. In a recent paper,[31] the authors observed a certain degree of occupational disorder in the crystal structure of the enantiopure 1-aza[6]helicene due to the position of the nitrogen. Therefore, we included in our calculations the cases with 'opposite' occupancy, where every helicene in the cell is rotated by 180° around its pseudo-C_2 symmetry axis (see Figure 1). Therefore, 16 different crystalline cells of monoaza[6]helicene isomers were considered. The geometry of each [6]helicene was manually created starting from the structure of the 6-aza[6]helicene in the crystal structure PIHDOB. Each helicene was then relaxed in vacuum with the semi-empirical AM1 method[32] followed by hybrid density-functional theory (B3LYP[33] with a 6-31G* basis set) with Gaussian09.[34] These geometries were projected back onto the crystallographic positions of the unit cell by the space group symmetry operations and translated by the lattice units to form a 3 × 3 × 3 supercell. For all of the structures in this work, the same experimental unit cell parameters of PIHDOB (6-aza[6]helicene) were used. The standard deviation of the cell lengths *a*, *b* and *c* for the isomers 1/2/6-aza for carbo[6]helicene in the CSD (codes: BAGLIH, BAGLED, PIHDOB and HEXHEL) are 0.0552, 0.0745 and 0.1834 Å respectively (see Table S1 for the complete list of cell lengths and Figure S1 to visualise the similarity between the cells). Therefore, supercells obtained by parameters of these isomers were expected to give reasonably close results.

This journal is © The Royal Society of Chemistry 20xx

Please do not adjust margins

Please do not adjust margins

Transfer integrals. The transfer integral *J* (also known as hopping integral or electronic coupling) represents the interaction energy between two molecular units associated with the charge transfer. We calculated the transfer integrals between each molecule in the central unit cell and all the other molecules in the supercell, subject to a distance cut-off of 15 Å. The transfer integrals were obtained with hybrid DFT molecular pair calculations and the projective method, which involves projecting the orbitals of the pair onto a basis set defined by the unperturbed orbitals of the individual molecules.[35] The Fock Matrix is rewritten in a new localised basis set using the orbital energies of the molecules pairs. The Fock matrix is then diagonalized to give the transfer integrals *J*. Molecular orbitals, energies and atomic orbital overlaps are obtained at the B3LYP/6-31G* level.

Reorganization energy. The reorganization energy is generally given by the sum of two terms: the inner (λ_{in}) and the outer reorganization energy (λ_{ou}).[36] The former reflects the energy cost associated with the geometrical relaxation of the single molecule undergoing reduction/oxidation, while the latter takes into account the modification of the surrounding crystal lattice. In this work, the outer reorganization energy is estimated at 0.3 eV for all the aza[6]helicene isomers. The inner part was computed for each aza[6]helicene isomer geometry optimised in the gas-phase at the B3LYP/6-31G* level in the neutral and the charged states through the 4-point method.[37] The total reorganization energy always remains higher than the transfer integrals, so we can apply the Marcus equation in the hopping regime.

Charge mobility prediction. Marcus theory is an established model of charge transport in organic small molecule semiconductors.[3] In this framework, the charge carrier is localised on a single molecule and moves to one of its neighbours by a 'hopping' mechanism, influenced by any local variations in site energy and electric fields. The charge transfer rate between two molecules, from which mobility is obtained, is related to the electronic coupling between the orbitals participating in the charge-transfer event, or transfer integral. In the approximation of frozen orbitals, the transfer integral is proportional to the overlap between the sole frontier orbitals of the two molecules, (HOMO or LUMO, respectively for hole and electron transfer). Larger charge-carrier mobilities are expected to result from large values of the transfer integral, but mobility is also affected by local variations in transfer integral, site energy and dimensionality. Here, the charge transfer rates between two units were calculated in the weak coupling limit ($J << \lambda_{tot}$) under an electric field of 10^4 V cm^{-1} using the Marcus equation.[14,38] The angular-dependent charge-carrier mobility was obtained through a master equation approach. Further details can be found in the SI.

Results and Discussion

Analysis of transfer integrals in typical packing motifs

In our analysis, neighbouring helicene pairs that showed transfer integrals lower than 1 meV were discarded, as it is reasonable to assume they do not contribute significantly to the charge transport. The remaining pairs could be grouped into 5 main packing motifs (shown in Figure 2): *T-shape (back)*, *Interlocked*, *T-shape (front)*, *Translational*, *Back-to-back*. In general, C-H···π interactions are more prevalent than π···π interactions. The shortest (~3 Å) and longest (~3.9 Å) C···C intermolecular distances are found for the *interlocked* and *T-shape (front)* motifs, respectively. Every helicene in the cell is involved exactly twice in each of the five packing motifs. As the *J* values in each instance are similar, the data shown here refer to the average of the two values.

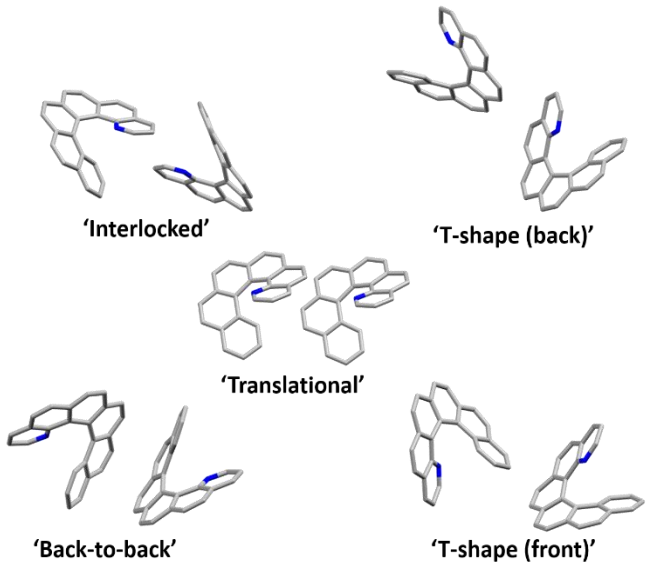


Figure 2. The five main motifs identified in the crystal structure analysed in this work. Note that every helicene has the (M) configuration. The nitrogen atoms are depicted in blue.

Eighteen supercells were considered: sixteen mono-aza[6]helicene regioisomers (the nitrogen position is indicated by numbers from 1 to 16 as in Figure 1 and referred to here onwards as ***x*-aza**), carbo[6]helicene and 1,16-diaza[6]helicene. It is important to stress that while the C_2-related isomers (**1-aza/16-aza**, **2-aza/15-aza** and so on so forth) are of course chemically identical, in the packing considered here, the interaction between the single helicene units is not the same. The handedness is not modified by rotation around the pseudo C_2 axis, so all the helicenes have the same chirality (M, left-handed). For each regioisomer of the series, the HOMO-HOMO and LUMO-LUMO transfer integrals of the five motifs are shown in Figure 3. The results have also been plotted separately for each motif in Figure S9. The highest transfer integrals were ~70 meV, lower than the transfer integrals calculated for stacked pentacenes, triphenylenes and other flat molecules.[39] On average, the energy of the transfer integrals is well below the total reorganization energy, which supports the use of a hopping model to describe the system.

In this work, we assume that the intermolecular distances for a given packing motif remain relatively unchanged regardless of the isomer considered. This is equivalent to saying that the relaxed geometry of the aza[6]helicenes is fairly rigid across the isomers series (small variations in pitch lengths are shown in Figure S2). However, since the transfer integrals are

Please do not adjust margins

Please do not adjust margins

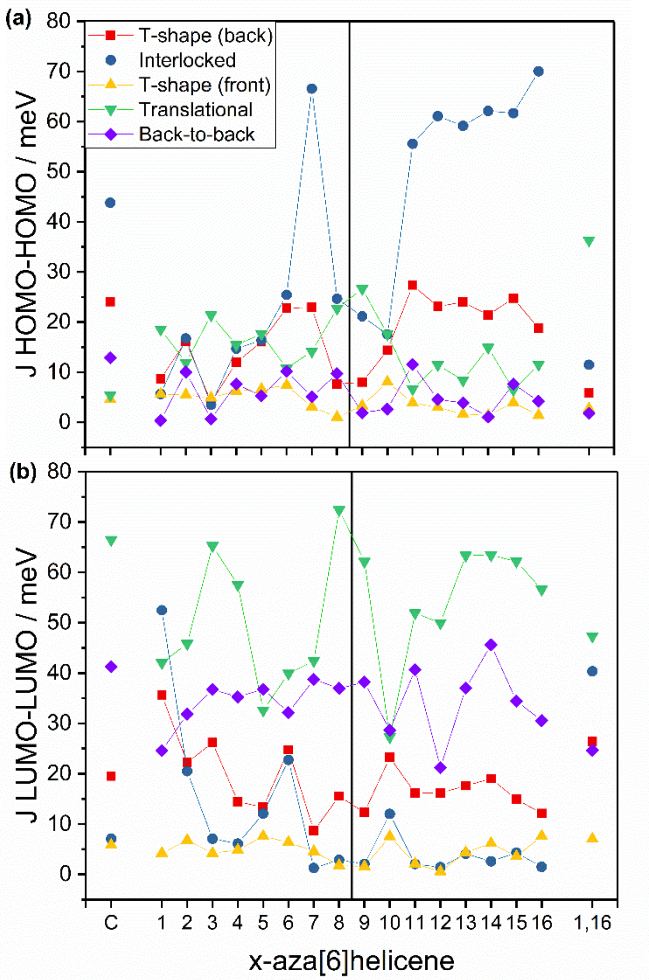


Figure 3. HOMO-HOMO (a) and LUMO-LUMO (b) transfer integrals calculated for every pair motif of each hypothetical structurel. The number on the *x*-axis indicates the position of the nitrogen in the aza[6]helicene scaffold. The entries C and 1,16 indicate the carbo[6]helicene (no nitrogens) and the 1,16-diaza[6]helicene, respectively.

known to scale exponentially with the intermolecular distance,[36] even small changes in the position of different isomers could in principle affect our analysis. To confirm whether allowing intermolecular changes would have significantly changed our results, we plotted the transfer integrals against the shortest intermolecular distances (C···C or C···N) of each interlocked pair, one of the most significant motifs for our analysis and the one with the highest variation in transfer integrals across systems. As we did not observe an exponential-like correlation (Figure S8), we consider the HOMO/LUMO distribution to play the dominant role in determining the charge transfer integrals. The intermolecular distance will be mentioned as a factor where applicable in the discussion of results.

The charge transfer is now discussed separately for each dimer motif:

Interlocked. With regard to the hole transfer (HOMO-HOMO *J*), the *interlocked* motif (blue dots in Figure 3) immediately stands out as having the highest values. The crystal **16-aza** showed the highest value of all the isomers considered (70 meV), for transport along the *b*-axis. The high coupling of this motif also leads to a particularly anisotropic hole transport, as can be seen in the angular-dependent hole mobility plots for **16-aza** in Figure 4. The second preferred direction in **16-aza** is the *a*-axis, along which holes can be transferred 'zig-zag' only through pairs of *interlocked* pairs.

The *interlocked* motif showed generally very high J values (55-70 meV) for the second half of the series from **11-aza** to **16-aza**, whereas they are quite low in the first half (with the exception of **7-aza**). This trend could be rationalised by

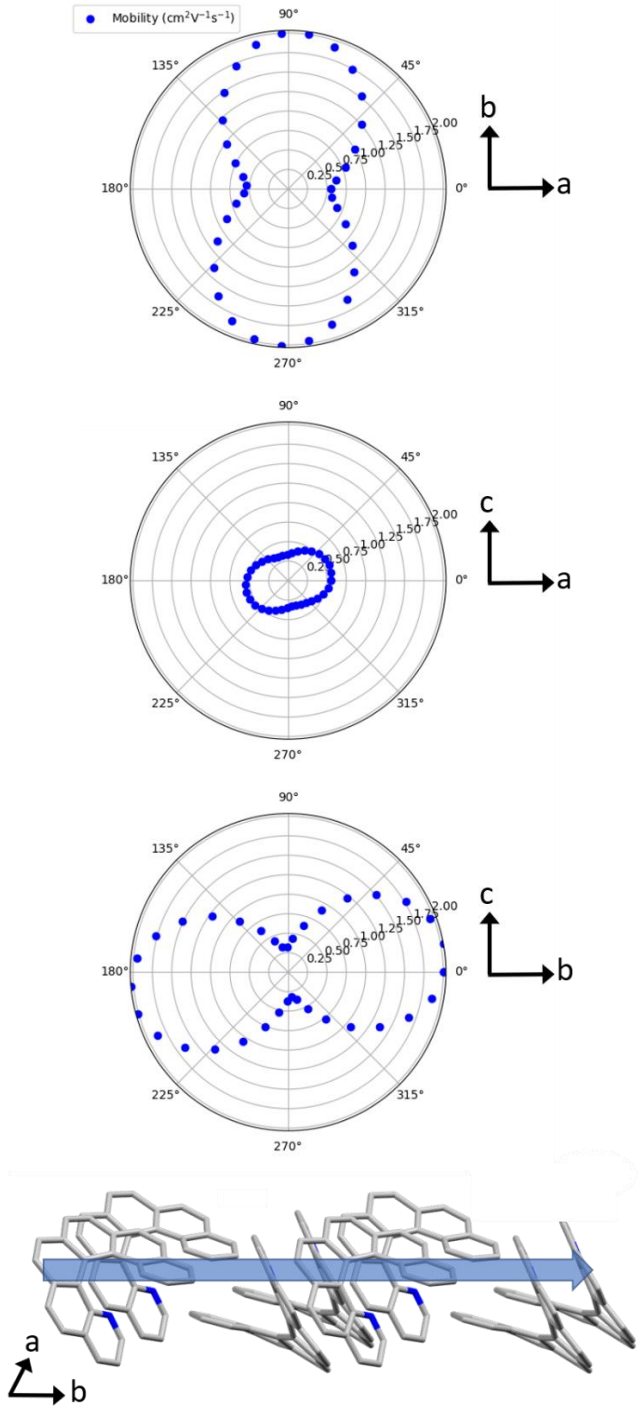


Figure 4. Angular-dependent hole mobility for **16-aza** in the three orthogonal planes (*ab*, *ac* and *bc*). Bottom: *Interlocked* and *back-to-back* motifs represented together for the **16-aza** cell. The *interlocked* pair is responsible for the high mobility along the *b*-axis. The blue arrow shows the highest hole-mobility direction.

This journal is © The Royal Society of Chemistry 20xx

Please do not adjust margins

Please do not adjust margins

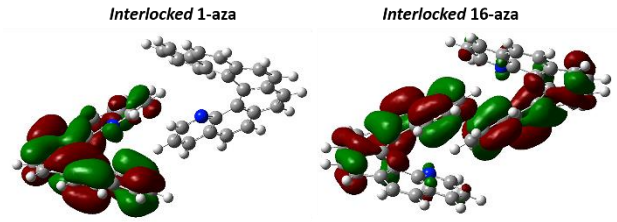


Figure 5. Representation of the HOMO for the *interlocked* pair in cells **1-aza** and **16-aza** (isovalue 0.02). The HOMO is localised only on one unit or delocalised over both units, respectively. This reflects the difference in hole transfer integrals between the two situations.

observing how the HOMOs of the single unit and the *interlocked* pairs are distributed for the different isomers (Figure S3).

The isomers from **1-aza** to **6-aza** present a similar situation; normally, the HOMO is mainly localized far from the ring bearing the nitrogen since this acts as an electron withdrawing group, reducing the electron density on the ring. An anomaly was found in **7-aza** where the HOMO distribution is almost inverted (*i.e.* it is localized close to the ring containing the nitrogen). The isomer **8-aza** shows a HOMO rather evenly distributed over the whole helicene scaffold due to the position of the nitrogen close to the pseudo C_2-axis of the molecule. The consequence is that in one case (for instance, **1-aza**) the HOMOs of two *interlocked* helicenes are further apart, resulting in poor hole transfer ($J \approx 5$ meV). Whereas, for the same isomer but opposite occupancy, **16-aza**, the different nitrogen position allows a better HOMO-HOMO overlap and much higher transfer integral ($J \approx 70$meV). The HOMO distribution of the *interlocked* pairs for **1-aza** and **16-aza** is shown in Figure 5, where the difference can be appreciated. The strong localisation of the HOMO in **1-aza** might be explained by the asymmetric arrangement of the molecules. It is known in literature that polarisation effects can cause an uneven distribution of the MOs when the molecules are not arranged symmetrically.[35,40] In this case, **1-aza** might experience a polarisation stronger than **16-aza** because of the proximity of the nitrogen atoms the **16-aza** pair (~5 *vs.* ~8 Å), leading to the greater degree of orbital asymmetry for **1-aza** than **16-aza** observed in Figure 5.

In line with the interpretation discussed above, the hole transfer integral for the *interlocked* pair of carbo[6]helicene (entry C in Figure 3) is about four times higher than in the 1,16-diaza[6]helicene. However, in this case, a visual inspection of the frontier orbitals does not provide further insight. Interestingly, the highest HOMO-HOMO integral of the cell of each isomer follows a similar trend to the transfer integrals of the *interlocked* helicene (see Figure S4a), supporting the importance of this motif in the crystal packing.

According to the discussion above, LUMO-LUMO integrals were expected to be higher in the first half of the isomer series, mirroring the hole transfer integral behaviour. In fact, electron transfer in the *interlocked* pairs was the highest for the isomer **1-aza** ($J \approx 52$ meV), followed by **1,16-diaza** ($J \approx 40$ meV), while the lowest values could be found from **11-aza** to **16-aza** (< 5 meV). Even the best LUMO-LUMO transfer integrals found were always lower than the highest HOMO-HOMO values.

From our analysis, we might expect that the HOMO-HOMO (LUMO-LUMO) transfer integral increases (decreases) with the nitrogen-nitrogen distance. However, Figure S7 does not show a clear trend between these two quantities, suggesting that other factors play an important role as well. In general, *interlocked* helicenes seemed to be particularly sensitive to the position of the nitrogen and the effect of the occupancy, possibly a consequence of the shortest intermolecular contact distance in the cell. It should also be highlighted that the *interlocked* motif is a quite common motif and present in the most thermodynamically stable polymorphs of [6]helicenes.[28]

Translational. This motif showed the highest LUMO-LUMO integrals for almost every isomer (between 30 and 75 meV) and reasonable but lower values of HOMO-HOMO integrals (where **1,16-diaza** was the best with 36 meV). This pair configuration was already found to be promising for electron transport in enantiopure crystals of [6]helicene,[28] and here we observe that this tendency seems not to be affected by the substitution of one or even two C-H vertex by nitrogen atoms. Furthermore, this motif lead to a very anisotropic charge transport with mobility of both charge carriers maximised along the *a*-axis due to the 'translated' arrangement of the helicenes (see Figure 4). For instance, **8-aza**, which shows the most efficient electron transfer in this motif (more than 30 meV higher than the other motifs), also has the highest anisotropy factor (Table S2 in SI).

T-shape (front). This arrangement of [6]helicene pairs has one of the lowest calculated *J* values (< 10 meV) for hole transfer (together with the *back-to-back* motif), regardless of the isomer considered. The LUMO-LUMO values were also the worst of all the motifs studied here. This might be due to the long intermolecular distances of these pairs (the shortest C···C distance being ~3.9 Å) as well as poor frontier orbital overlap. The latter is indeed expected to decrease for a T-shaped interaction between aromatic systems, compared to face to face π-π stacking motifs.[41,42] When optimising helicene organic semiconducting materials, it would be desirable to have helicene crystal packings that do not include this motif, if possible, if one wants to maximise charge carrier mobility in all dimensions.

Back-to-back. This motif was one of the worst in terms of hole transfer integrals but showed the second-best values for electron transport. No clear trend related to the position of the nitrogen in the aromatic scaffold was observed. The shortest C···C distance in this motif is found to be ~3.4-3.6 Å, an intermediate case between the *interlocked* and *T-shape(front)* case. This shows again how, for a given arrangement and distance between two helicenes, transfer integrals for hole and electron can be very different because of the frontier orbitals' spatial organisation.

T-shape (back). Transfer integrals for this motif were found in the range between 10 and 30 meV for both charge carriers. Differences between opposite occupancy could be observed, however the effect here is much less pronounced than in the *interlocked* motif, probably due to the longer intermolecular distances.

Overall, the substitution of a C-H vertex with a nitrogen atom (or even two) in the aromatic scaffold of the [6]helicene was not found to provide particular advantages in terms of

This journal is © The Royal Society of Chemistry 20xx

Please do not adjust margins

Please do not adjust margins

electron or hole transfers. For all the motifs, hole transfer was generally lower in the aza[6]helicenes than in the carbo[6]helicene. The only significant exception lies in the pair of *interlocked* helicenes, which can show improved transfer integrals (HOMO-HOMO or LUMO-LUMO) as long as the nitrogen occupancy is 'correct' - *i.e.* the nitrogen atoms of neighbouring helicenes are positioned on rings close or far from each other depending on the charge carrier. From an experimental viewpoint, these observations indicate that the device mobility could potentially be tuned by the occupational order in the crystal, that is the nitrogen position with respect to the pseudo-C_2 axis of the hexahelicene. However, building crystal structures with a targeted occupancy pattern is currently, to the best of our knowledge, nearly impossible. Therefore, an average value between those of the two opposite occupancies would most likely be achieved.

Charge mobility

The transfer integrals calculated were applied in the Marcus equation to obtain the orientation-dependent charge mobility of holes and electrons in the supercells (as models of the corresponding single crystal) for all isomers. It is important to keep in mind that the absolute values of charge mobility depend on the total reorganization energy employed to describe the system. Therefore, we focused on analysis across the series of aza[6]helicene isomers. Since the reorganization energy acts as a scaling factor and we used a consistent method, we can analyse the comparison of the charge mobility values between the crystalline cells across the aza[6]helicene series. A comparison with experimental values is not possible due to the absence of literature data for these systems.

In general, high transfer integrals do not imply necessarily good charge mobility, as the former is defined for a molecular pair and the latter depends on a preferential pathway across a complete unit cell of pair interactions. If *J* for a dimer is too high compared to the surrounding dimers, the charge can be kinetically trapped, not achieving the best possible transport. However, in this study, we found that the maximum transfer integrals correlate quite well with the maximum and average charge mobility (see Figures S5a and S5b). A relationship could be found between the HOMO-HOMO (LUMO-LUMO) transfer integrals of the *interlocked* (*translational)* and the average or maximum hole mobility (Figures S6c and S6d). This supported the central role of these two packing motifs for hole and electron transport respectively.

The average hole mobility graph (Figure 6a) shows a comparable trend to that we explored above: a quite significant disparity between isomers from **1-aza** to **7-aza** and their C_2-related isomers from **10-aza** to **16-aza** (see Figure S5a and S5c to visualise more clearly). In the first half of the series, the calculated average hole mobility is lower than 0.05 $cm^2\ V^{-1}\ s^{-1}$ while in the second half it goes from 0.07 to 0.12 $cm^2\ V^{-1}\ s^{-1}$. The only exceptions are, again, given by the pair **7-aza**/**10-aza**, where the tendency is inverted, and the pair **8-aza**/**9-aza**, where the values are very similar to each other. The average hole mobility of this crystal packing seems mainly driven by the efficiency of the hole transfer in the *interlocked* motif. This is important, as it helps to create rules for the chemical design of novel helicene structures with improved hole mobility.

The trend in the hole mobility discussed so far did not apply for electron mobility. The results suggest the occupancy is not a critical factor, since C_2-related isomers present similar values of average and maximum electron mobility (Figure S5b and S5d). The only exception is the **1-aza/16-aza** pair, for which a 75% difference in the average electron mobility for **1-aza** compared to **16-aza** was found against a difference lower than 23% in the other opposite occupancy pairs (Figure S5d).

The information shown so far were obtained in order to elucidate the relation between nitrogen substitution pattern and charge transport in enantiopure [6]helicenes crystals. To assist with the visualization of the data, we constructed polar plots, shown in Figure 7. The anisotropy here is calculated as the normalised standard deviation of the direction-dependent mobility values (*i.e.* divided by the maximum value). In the plots, the four characteristics (maximum mobility, average mobility, anisotropy and reorganization energy) are converted into a normalised fitness parameter spanning linearly from 0 (worst

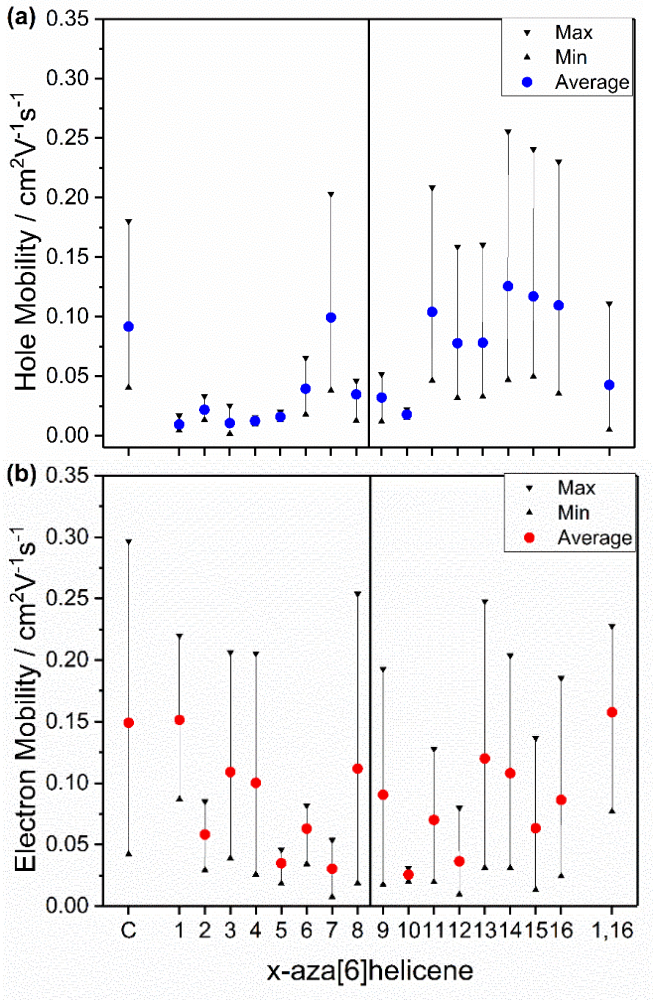


Figure 6. Maximum, minimum and average hole (a) and electron (b) mobility values calculated for each structure. The number of the *x*-axis entries indicates the position of the nitrogen in the aza[6]helicene scaffold. The entries C and 1,16 indicate the carbo[6]helicene (no nitrogen) and the 1,16-diaza[6]helicene, respectively.

This journal is © The Royal Society of Chemistry 20xx

Please do not adjust margins

value) to 1 (best value), assuming one tries to maximise the highest and average mobility and minimise anisotropy and reorganization energy. For applications as field-effect transistors, a low anisotropy is normally advisable to achieve more reproducible performances as controlling the orientation of the crystalline domains in thin film is challenging. All the calculated values can be found in the supporting information file (Table S2).

At first sight, none of the candidate [6]helicenes analysed here seems to be endowed with all the best characteristics at the same time. The isomers showing high average and maximum mobility are also characterized by strong anisotropy. The preferred mobility directions are, almost invariably for any isomer, the *a* and *b*-axis, respectively for electron and hole transport (an important exception being **1,16-diaza** where the *a*-axis is preferred for both carriers). One could in theory take advantage of this feature to achieve orthogonal ambipolar charge transport by orienting properly the crystal or thin film on the transistor substrate.

For hole transport, average mobility seems to correlate only weakly with the reorganization energy, while these quantities correlate quite well for the electron transport. The effect of multiple nitrogen substitution on the reorganization energy has been previously studied in pentacene.[43] λ_{in} was found to increase with the number of nitrogen substitutions. In our case, despite only a low degree of substitution being considered, the effect on the reorganization energy is not monotonic. The substitution of a single nitrogen atom increased the reorganization energy, regardless of the position, whilst two nitrogen atoms lead to the lowest value in the table for both hole and electron transfer. **1,16-diaza** also showed the highest average electron mobility (0.158 $cm^2\ V^{-1}\ s^{-1}$), although only slightly above the carbo[6]helicene, which would make it an interesting electron transport target material.

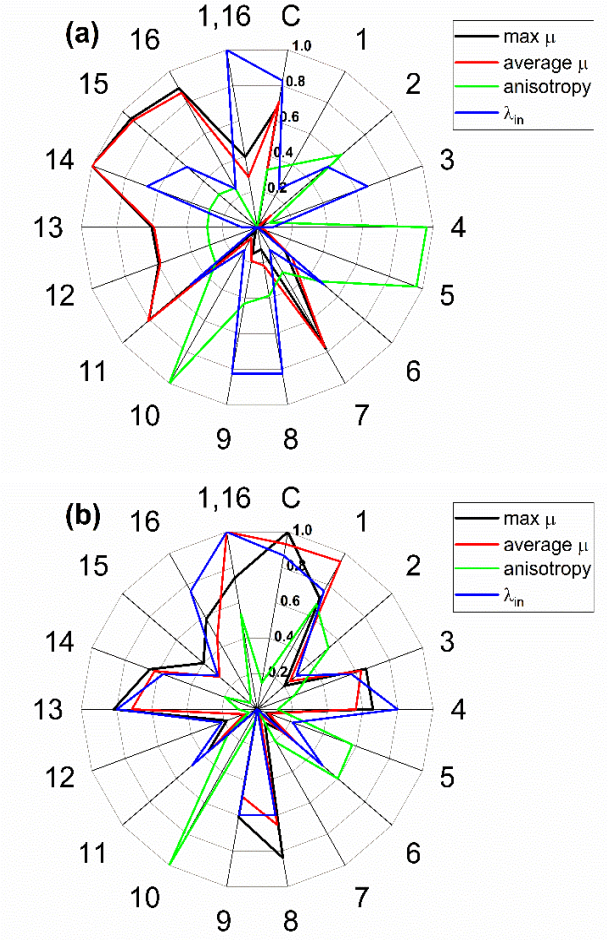


Figure 7. Polar plot of fitness parameters associated to hole (a) and electron (b) transport. 1 (0) corresponds to the best (worst) characteristic amongst all the structures studied in this work. Normalised values are calculated as $x_{norm} = (x - x_{min})/(x_{max} - x_{min})$ for max μ and average μ and as $1 - x_{norm}$ for anisotropy and λ_{in}. The entries indicate the position of the nitrogen in the aza[6]helicene scaffold. C and 1,16 indicate the carbo[6]helicene (no nitrogen) and the 1,16-diaza[6]helicene, respectively.

Conclusions

We have studied the relationship between the chemical structure of a series of aza[6]helicenes and the charge carrier mobility in a crystal cell. The packing chosen is one of the most thermodynamically stable for enantiopure [6]helicenes. The simulations showed that, for the same solid-state packing, the position of the nitrogen in the aromatic scaffold can be crucial in determining the semiconducting properties of the material. Moreover, through studying the transfer integrals, we were able to identify supramolecular motifs which are promising or have a central role in promoting high hole and electron transport, the *interlocked* and *translational* motifs respectively. For both motifs, transfer integrals can reach values as high as 70 meV. This can cause a difference in the charge mobility between the best and the worst crystal cells of up to one order of magnitude. These results can hopefully contribute to the understanding of the semiconducting properties of helical organic molecules.

While the trend in the *interlocked* hole transfer integrals can be explained partially by the visualization of the HOMO orbitals, the strong impact on the hole mobility could not be easily foreseen. From the experimental point of view, the synthesis and characterisation of several helicene derivatives would be an extremely demanding task. The much shorter time required for calculations allows one to obtain more detailed information on structure-property relationships in these systems, which is useful for the design of new helicene-based materials.

Conflicts of interest

There are no conflicts to declare.

Acknowledgements

The authors thank the EPSRC for funding (EP/M017257/1, EP/N004884/1, EP/L016702/1, EP/P000525/1, EP/L014580/1, EP/P005543/1 and EP/R00188X/1). K. E. J. thanks the Royal Society for a University Research Fellowship and an Enhancement Award (J.S.) and the ERC through grant agreement number 758370 (ERC-StG-PE5- CoMMaD). J. N. thanks the ERC for support under the European Union's Horizon 2020 research and innovation program (Grant Agreement No

Please do not adjust margins

742708). We thank Dr. Jochen R. Brandt for valuable discussions.

Notes and references

1 L. Li, W. Hu, H. Fuchs and L. Chi, *Adv. Energy Mater.*, 2011, **1**, 188–193.

2 X. Feng, V. Marcon, W. Pisula, M. R. Hansen, J. Kirkpatrick, F. Grozema, D. Andrienko, K. Kremer and K. Müllen, *Nat. Mater.*, 2009, **8**, 421–426.

3 D. T. James, J. M. Frost, J. Wade, J. Nelson and J. S. Kim, *ACS Nano*, 2013, **7**, 7983–7991.

4 M. Klues and G. Witte, *CrystEngComm*, 2018, **20**, 63–74.

5 J. R. Brandt, F. Salerno and M. J. Fuchter, *Nat. Rev. Chem.*, 2017, **1**, 0045.

6 R. Naaman and D. H. Waldeck, *Annu. Rev. Phys. Chem.*, 2015, **66**, 263–281.

7 M. Gingras, *Chem. Soc. Rev.*, 2013, **42**, 1051–1095.

8 Y. Shen and C.-F. Chen, *Chem. Rev.*, 2012, **112**, 1463–1535.

9 C.-F. Chen and Y. Shen, *Helicene Chem. from Synth. to Appl.*, 2017, **XIV**, 19–40.

10 C. Kim, T. J. Marks, A. Facchetti, M. Schiavo, A. Bossi, S. Maiorana, E. Licandro, F. Todescato, S. Toffanin, M. Muccini, C. Graiff and A. Tiripicchio, *Org. Electron. physics, Mater. Appl.*, 2009, **10**, 1511–1520.

11 A. Irfan, M. Assiri and A. G. Al-Sehemi, *Org. Electron.*, 2018, **57**, 211–220.

12 L. Shi, Z. Liu, G. Dong, L. Duan, Y. Qiu, J. Jia, W. Guo, D. Zhao, D. Cui and X. Tao, *Chem. - A Eur. J.*, 2012, **18**, 8092–8099.

13 Y. Yang, R. C. da Costa, M. J. Fuchter and A. J. Campbell, *Nat. Photonics*, 2013, **7**, 634–638.

14 Y. Yang, B. Rice, X. Shi, J. R. Brandt, R. Correa da Costa, G. J. Hedley, D.-M. Smilgies, J. M. Frost, I. D. W. Samuel, A. Otero-de-la-Roza, E. R. Johnson, K. E. Jelfs, J. Nelson, A. J. Campbell and M. J. Fuchter, *ACS Nano*, 2017, **11**, 8329–8338.

15 T. Hatakeyama, S. Hashimoto, T. Oba and M. Nakamura, *J. Am. Chem. Soc.*, 2012, **134**, 19600–19603.

16 S. Jhulki, A. K. Mishra, T. J. Chow and J. N. Moorthy, *Chem. - A Eur. J.*, 2016, **22**, 9375–9386.

17 L. Shi, Z. Liu, G. Dong, L. Duan, Y. Qiu, J. Jia, W. Guo, D. Zhao, D. Cui and X. Tao, *Chem. - A Eur. J.*, 2012, **18**, 8092–8099.

18 P. Josse, L. Favereau, C. Shen, S. Dabos-Seignon, P. Blanchard, C. Cabanetos and J. Crassous, *Chem. - A Eur. J.*, 2017, **23**, 6277–6281.

19 C. Li, Y. Yang and Q. Miao, *Chem. - An Asian J.*, 2018, **13**, 884–894.

20 A. J. Lovinger, C. Nuckolls and T. J. Katz, *J. Am. Chem. Soc.*, 1998, **120**, 264–268.

21 O. Ermer and J. Neudörfl, *Helv. Chim. Acta*, 2001, **84**, 1268–1313.

22 K. Nakano, H. Oyama, Y. Nishimura, S. Nakasako and K. Nozaki, *Angew. Chemie Int. Ed.*, 2012, **51**, 695–699.

23 P. Rahe, M. Nimmrich, A. Greuling, J. Schütte, I. G. Stará, J. Rybáček, G. Huerta-Angeles, I. Starý, M. Rohlfing and A. Kühnle, *J. Phys. Chem. C*, 2010, **114**, 1547–1552.

24 S. L. Price, *Chem. Soc. Rev.*, 2014, **43**, 2098–111.

25 G. M. Day and A. I. Cooper, *Adv. Mater.*, 2017, **30**, 1704944.

26 J. E. Campbell, J. Yang and G. M. Day, *J. Mater. Chem. C*, 2017, **5**, 7574–7584.

27 F. Musil, S. De, J. Yang, J. E. Campbell, G. M. Day and M. Ceriotti, *Chem. Sci.*, 2018, **9**, 1289–1300.

28 B. Rice, L. M. LeBlanc, A. Otero-de-la-Roza, M. J. Fuchter, E. R. Johnson, J. Nelson and K. E. Jelfs, *Nanoscale*, 2018, **10**, 1865–1876.

29 A. Matsumoto, K. Yonemitsu, H. Ozaki, J. Míšek, I. Starý, I. G. Stará and K. Soai, *Org. Biomol. Chem.*, 2017, **15**, 1321–1324.

30 E. Kaneko, Y. Matsumoto and K. Kamikawa, *Chem. - A Eur. J.*, 2013, **19**, 11837–11841.

31 J. R. Brandt, L. Pospíšil, L. Bednárová, R. C. da Costa, A. J. P. White, T. Mori, F. Teplý and M. J. Fuchter, *Chem. Commun.*, 2017, **53**, 9059–9062.

32 M. J. S. Dewar, E. G. Zoebisch, E. F. Healy and J. J. P. Stewart, *J. Am. Chem. Soc.*, 1985, **107**, 3902–3909.

33 A. D. Becke, *J. Chem. Phys.*, 1993, **98**, 5648–5652.

34 G. E. S. M. J. Frisch, G. W. Trucks, H. B. Schlegel, V. B. M. A. Robb, J. R. Cheeseman, G. Scalmani, G. Z. B. Mennucci, G. A. Petersson, H. Nakatsuji, M. Caricato, X. Li, H. P. Hratchian, A. F. Izmaylov, J. Bloino, R. F. J. L. Sonnenberg, M. Hada, M. Ehara, K. Toyota, O. K. J. Hasegawa, M. Ishida, T. Nakajima, Y. Honda, J. E. P. H. Nakai, T. Vreven, J. A. Montgomery Jr., E. N. B. F. O. Ogliaro, M. J. Bearpark, J. Heyd, J. N. K. N. Kudin, V. N. Staroverov, R. Kobayashi, S. S. I. K. Raghavachari, A. P. Rendell, J. C. Burant, M. K. J. Tomasi, M. Cossi, N. Rega, N. J. Millam, J. J. J. E. Knox, J. B. Cross, V. Bakken, C. Adamo, A. J. A. R. Gomperts, R. E. Stratmann, O. Yazyev, R. L. M. R. Cammi, C. Pomelli, J. W. Ochterski, P. S. K. Morokuma, V. G. Zakrzewski, G. A. Voth, A. D. D. J. J. Dannenberg, S. Dapprich, J. C. Ã. D. N. Farkas, J. B. Foresman, J. V. Ortiz and and D. J. Fox, 2009.

35 J. Kirkpatrick, *Int. J. Quantum Chem.*, 2008, **108**, 51–56.

36 J. L. Brédas, D. Beljonne, V. Coropceanu and J. Cornil, *Chem. Rev.*, 2004, **104**, 4971–5003.

37 V. Lemaur, A. Demetrio, S. Filho, V. Coropceanu, M. Lehmann, Y. Geerts, J. Piris, M. G. Debije, A. M. Van De Craats, K. Senthilkumar, L. D. A. Siebbeles, J. M. Warman, J. Bre and L. De Chimie, *JACS*, 2004, 3271–3279.

38 R. A. Marcus, *J. Chem. Phys.*, 1956, **24**, 966–978.

39 K. Senthilkumar, F. C. Grozema, F. M. Bickelhaupt and L. D. A. Siebbeles, *J. Chem. Phys.*, 2003, **119**, 9809–9817.

40 E. F. Valeev, V. Coropceanu, D. A. Da Silva Filho, S. Salman and J. L. Brédas, *J. Am. Chem. Soc.*, 2006, **128**, 9882–9886.

41 Y. R. Shi, H. L. Wei, X. B. Jia and Y. F. Liu, *J. Mater. Sci.*, 2018, **53**, 15569–15587.

42 G. R. Hutchison, M. A. Ratner and T. J. Marks, *J. Am. Chem. Soc.*, 2005, **127**, 16866–16881.

43 H. Chen and I. Chao, *ChemPhysChem*, 2006, **11528**, 2003–2007.

This journal is © The Royal Society of Chemistry 20xx

Please do not adjust margins